12th International Conference on Fracture Mechanics of Concrete and Concrete Structures
FraMCoS-12
B.L.A. Pichler, Ch. Hellmich, P. Preinstorfer (Eds)

https://doi.org/10.21012/FC12.1212
MS07-1:2

# FACTORS AFFECTING THE INTERFACIAL HEALING BETWEEN A FIBER AND CEMENT

**REINA NETTE R. DAGUIO[*] AND JISHEN QIU[†]**

Hong Kong University of Science and Technology, Department of Civil and Environmental Engineering
Clear Water Bay, Hong Kong, China
[*] e-mail: rnrdaguio@ust.hk
† e-mail: cejqiu@ust.hk

**Key words:** Interface bond, Autogenous healing, Natural fiber, PVA, Reactive magnesia cement, Single-fiber pullout test

**Abstract:** The mechanical performance of fiber-reinforced cementitious composites (FRCCs) significantly depends on the strength of the interface bond between the fibers and the cement matrix. An important aspect that can affect the properties of the fiber-matrix interface is interfacial healing – a process wherein the interface undergoes repair after being damaged. In this study, we investigate the interfacial healing efficiency of mechanically preloaded and then environmentally conditioned specimens using the single-fiber pullout test. In the experimental setup, single-fiber specimens were subjected to preloading to induce damage, followed by environmental conditioning to promote interfacial healing. The effectiveness of the healing process was assessed by performing the single-fiber pullout test on the healed specimens. For comparison, specimens that were not preloaded but subjected to identical environmental conditions were also evaluated. The bond strength and interface bond recovery of the specimens were quantitatively assessed.

## 1 INTRODUCTION

Fiber-reinforced cementitious composites (FRCCs) have become increasingly popular in the construction industry because they offer better mechanical properties than traditional concrete. Adding fibers to cement matrices enhances tensile strength, ductility, toughness, and crack resistance, making these materials particularly advantageous for various structural applications [1]. The overall performance of FRCCs largely depends on the bond strength at the interface between the reinforcing fibers and the cement matrix. This interface bond strength is critical for successfully transferring stress between the fiber and the matrix during mechanical loading, and it plays a role in maintaining the structural integrity of the composite [2]. The interfacial healing process, which repairs damage at the fiber-matrix interface, can recover the bond strength and improve the composite's durability [3]. This process is influenced by the fiber type, matrix properties, environmental conditions, and the extent of damage.

Different types of fibers, such as natural sisal fibers and synthetic polyvinyl alcohol (PVA) fibers, have distinct compositions and microstructural features that can significantly affect the properties of the fiber-matrix interface bond. Natural fibers, derived from plants, consist of hollow tubular structures known as lumens and are hygroscopic, which leads to dimensional instability due to swelling or shrinkage depending on the environmental condition [4]. This instability can adversely affect the mechanical performance of the composite [5]. On the other hand, synthetic PVA fibers are solid, hydrophilic, and known to

bond well with cementitious materials [6]. These differences in physical and chemical properties necessitate a thorough investigation into how they influence the autogenous healing of the fiber-matrix interface.

The type of matrix also affects the healing process. Reactive magnesia cement (RMC) is an emerging sustainable binder due to its ability to sequester carbon dioxide ($CO_2$) [7]. When the magnesium oxide (MgO) reacts with water, brucite ($Mg(OH)_2$) is formed. The brucite can then react with $CO_2$ to produce hydrated magnesium carbonates (HMCs) which are mainly responsible for the strength of the cement matrix [8]. However, the depth of carbonation in RMC is limited because its dense microstructure hinders $CO_2$ penetration [9]. This issue can be addressed by adding hollow natural fibers, which consist of lumens that serve as tunnels for $CO_2$ to penetrate deeper into the RMC matrix, thereby improving $CO_2$ sequestration and strength [10].

The healing degree at the fiber-matrix interface can be assessed using the single-fiber pullout test, which allows for the quantification of bond strength recovery of a debonded-and-healed interface and provides insights into the effectiveness of the environmental conditioning process. It was found that Sisal-RMC specimens exhibited better chemical and frictional bond recovery compared to PVA-RMC and PVA-PC specimens when subjected to alternating water/air conditioning [11]. For PVA-PC specimens, the alternating water/air conditioning promotes frictional bond strength recovery but does not restore the chemical bond at the debonded interface [12]. Research on the autogenous healing of PVA-RMC composites has shown that exposure to alternating water/$CO_2$ conditioning results in more effective healing that is less dependent on the preloading level compared to those that are exposed to alternating water/ambient air conditioning. However, the study focused on the healing of cracks in composites [13]. Previous studies have not investigated the use of alternating water/$CO_2$ conditioning to promote the fiber-matrix interface healing in RMC matrix with either synthetic or natural fibers, but especially hollow natural fibers.

This study examines the interface healing of Sisal-RMC and PVA-RMC specimens after debonding and healing through alternating water/$CO_2$ conditioning. Natural sisal fibers and synthetic PVA fibers were chosen due to their differing properties, which may influence the healing process at the fiber-matrix interface. PVA fibers are known for their strong chemical bonding capabilities with cement matrices, while sisal fibers provide environmental benefits, albeit with potential drawbacks such as dimensional instability. This research aims to provide insights into the factors affecting the interfacial healing process, which is essential for optimizing the performance of FRCCs and developing sustainable construction materials.

## 2 EXPERIMENTAL PROGRAM

### 2.1 Summary

The single-fiber pullout test was performed to evaluate the fiber-matrix interface properties under various conditions: 1) after curing, 2) after a “healing” process without preloading, and 3) after preloading followed by healing. During the healing process, the specimens underwent five cycles of water/$CO_2$ conditioning. Each cycle consisted of 12 hours of immersion in water at room temperature, followed by 12 hours in a carbonation chamber (30±2°C, 85±5% relative humidity, 10% $CO_2$ concentration).

### 2.2 Raw materials

The reactive magnesia cement (magnesium oxide light, STARMAG 150) was sourced from Konoshima Chemical Co., Ltd. The properties of the cement, as provided by the manufacturer, are detailed in Table 1. Sodium hexametaphosphate (SHMP), which was used to enhance the workability of the cement paste [14], was obtained from Xilong Chemistry Ltd.

In this study, both natural sisal fibers and synthetic polyvinyl alcohol (PVA) fibers were utilized. The continuous sisal fibers, sourced from Zhejiang Rafi Grass Paper Products Co., Ltd., were cut to a length of 100mm. The PVA fibers (Grade No. RFS400), 18mm in length, were supplied by Kuraray Ltd. The properties

of these fibers are summarized in Table 2.

**Table 1**: Properties of the reactive magnesia cement from Konoshima Chemical Co., Ltd.

| | |
|---|---|
| Loss of ignition | 7% |
| Assay as MgO (Ignited basis) | 97.5% |
| Calcium Oxide | 0.7% |
| Iron | 0.02% |
| Specific surface area | 145$m^2/g$ |
| Average particle size | 3.5μm |

**Table 2**: Properties of the sisal and PVA fibers

| Property | Sisal Fiber | PVA Fiber |
|---|---|---|
| Length (mm) | 100 | 18 |
| Diameter (μm) | 235-560 | 200 |
| Tensile strength (MPa) | ~257 | 975 |
| Young's modulus (GPa) | ~3.5 | 27 |

## 2.3 Specimen preparation

A cement block, with multiple fibers sticking out, was fabricated using a mold that included one base plate and two additional 2mm thick plates placed on top of the base plate. These top plates were used to secure the fibers in place and to shape the 80mm x 10mm x 4mm cement block. The ends of the fibers were taped between these two top plates. After securing the fibers, the fresh cement paste can be poured into the mold. The fresh cement paste has a water-to-RMC ratio and SHMP-to-water ratio of 0.73 and 0.1 by weight, respectively.

After preparing the molds and weighing the raw materials, the mixing and casting procedures were carried out as follows: 1) the SHMP was dissolved into the mixing water 2) the RMC was placed in a planetary mixer and the SHMP solution was gradually poured, and mixed for three minutes. To ensure that a homogeneous cement paste is achieved, hand mixing was also performed. This involves scraping the bottom and sides of the mixer to fully incorporate all materials. 3) The RMC paste was poured into the molds. Each mold was tapped lightly on the laboratory bench to release any trapped air bubbles. The molds were kept in ambient air for 24 hours before being demolded.

After demolding, the cement block was cut using a diamond precision saw (IsoMet™ 1000 precision sectioning saw, Buehler Ltd.) to produce single-fiber specimens with a thickness of 3±0.5mm, which corresponds to the embedment length of the fiber. Finally, the single-fiber specimens were cured in a carbonation chamber (30±2°C, 85±5% relative humidity, 10% $CO_2$ concentration) for 24 hours.

## 2.4 Single-fiber pullout test

To conduct the single-fiber pullout test, a universal testing machine (EZ50, Lloyd Instruments) with a 20N load cell and displacement-controlled actuator was utilized. The single-fiber specimen was mounted by gluing it onto a metal block. The cross-section of the fiber at the bottom of the specimen was covered with tape to prevent the glue from interfering with the pullout test. The metal block was then placed on top of an X-Y table, carefully aligning the specimen so that the fiber and the clamp were in proper alignment. The fiber was securely clamped, and the X-Y table was used to fine-tune the position of the specimen to ensure that the fiber axis was perpendicular to the surface of the specimen. After installing the specimen, a tensile load was applied at a loading rate of 0.5mm/min, and the load ($P$) versus displacement ($\delta$) curves were recorded.

For the first group of specimens, the monotonic load was applied right after curing. For the second group, the monotonic load was applied after curing and "healing" without preloading. For the third group, monotonic preloading was applied after curing. During the preloading, the load versus displacement graph was closely monitored. The preloading was stopped as soon as a load drop was detected, indicating that the fiber had completely debonded from the matrix [15]. Following this, the specimens were exposed to five cycles of water/$CO_2$ conditioning intended to promote healing at the fiber-matrix interface. After the healing process, a final monotonic reloading

was conducted to pull the fiber entirely out of the matrix. The interface properties of each group were determined based on data from at least three representative specimens.

## 3 RESULTS AND DISCUSSIONS

In the initial stage of the single-fiber pullout test, the fiber-matrix interface undergoes debonding. The tensile load applied to the fiber causes a displacement that can be attributed to the elastic stretching of the debonded segment as well as the free length of the fiber [15]. As the load increases, the chemical bond gradually gets broken and the length of the debonded segment progressively increases until it reaches the embedded end of the fiber (i.e., the length of the debonded segment equals the embedded length of the fiber). When complete debonding occurs, a maximum debonding load $P_a$ is reached and then the load suddenly drops to the initial frictional pullout load $P_b$. The drop in load, which stops at $P_b$ due to friction at the interface, marks the transition from the fiber debonding stage to the fiber slippage stage. During the latter stage, the fiber begins to slide out of the matrix tunnel, and the slippage is resisted by the friction between the fiber and the matrix. After the fiber is completely pulled out, the resulting load-displacement curve from the single-fiber pullout test can be used to determine the fiber-matrix interface properties. A typical load-displacement curve is presented in Figure 1.

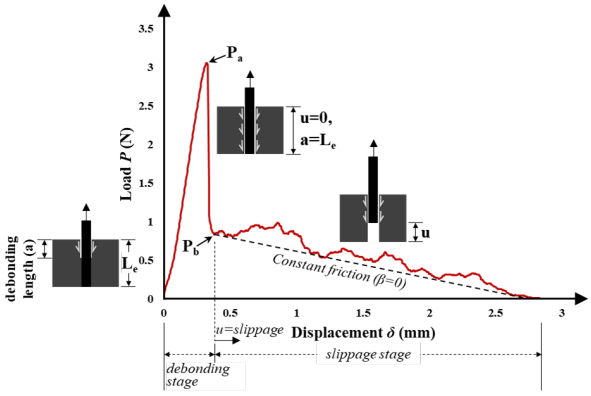


**Figure 1**: Typical single-fiber pullout curve

The chemical bond $G_d$ represents the energy required to completely debond the fiber from the matrix while the frictional bond $\tau_o$ quantifies the fiber's initial resistance to slippage. These interface properties are calculated using the following equations [15]:

$$G_d = \frac{2(P_a - P_b)^2}{\pi^2 E_f d_f^3} \text{ (J/m}^2\text{)} \quad (1)$$

$$\tau_o = \frac{P_b}{\pi d_f L_e} \text{ (MPa)} \quad (2)$$

where $E_f$ is the Young's modulus of the fiber, $d_f$ is the fiber diameter, and $L_e$ is the fiber embedment length.

The slip-hardening coefficient $\beta$ accounts for the change in frictional resistance as the fiber is being pulled out from the matrix. It can be inversely calculated based on the value of $G_{w\_1}$ [16]. $G_{w\_1}$ quantifies the energy absorbed (or work done) per interface area to achieve 1mm displacement during the pullout process. The equation used to calculate $G_{w\_1}$ is as follows [11]:

$$G_{w\_1} = \frac{\int_0^1 P(\delta)\, d\delta}{\pi d_f L_e} \text{ (J/m}^2\text{)} \quad (3)$$

The fiber-matrix interface properties were calculated based on the load-displacement curves obtained under various conditions: 1) immediately after curing, 2) after "healing" without preloading, and 3) after preloading, healing then final reloading, as illustrated in Figure 2.

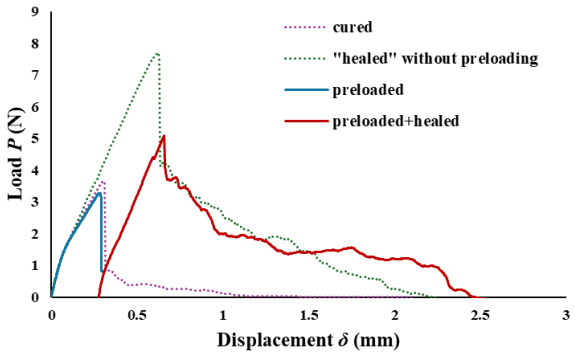


**Figure 2**: Example of single-fiber pullout curves used to determine the interface properties

For the preloaded specimen, $G_d$ and $\tau_o$ were calculated twice (before and after healing) to verify that the interface properties of the preloaded specimens were comparable with those of the specimens tested immediately after curing. This approach ensures that the interface

properties of the preloaded-and-healed specimens can be directly compared with the specimens that were only cured. Thus, the degree of healing can be quantified by dividing the interface properties of the preloaded-and-healed specimens by those of the cured specimens.

The interface properties of Sisal-RMC and PVA-RMC specimens are shown in Figures 3 to 6. Figure 3 compares the chemical bond $G_d$ for both fiber types across different conditions. It shows that PVA-RMC specimens typically have higher $G_d$ values in all conditions except when healed after preloading, where Sisal-RMC exhibits a higher $G_d$. This could be attributed to the chemical and physical properties of PVA fibers which may form a more effective bond with the matrix initially. The alternating water/$CO_2$ conditioning increased the $G_d$ of both non-preloaded PVA-RMC and Sisal-RMC specimens. However, the preloaded-and-healed PVA-RMC has a lower $G_d$ than the cured PVA-RMC, indicating that the chemical bond of PVA-RMC cannot be fully reestablished after debonding. The same was observed in a study that tested PVA-PC specimens [12]. On the other hand, the preloaded-and-healed Sisal-RMC has a higher $G_d$ than the cured Sisal-RMC, signifying that alternating water/$CO_2$ conditioning can reestablish and even improve the chemical bond between a sisal fiber and RMC matrix.

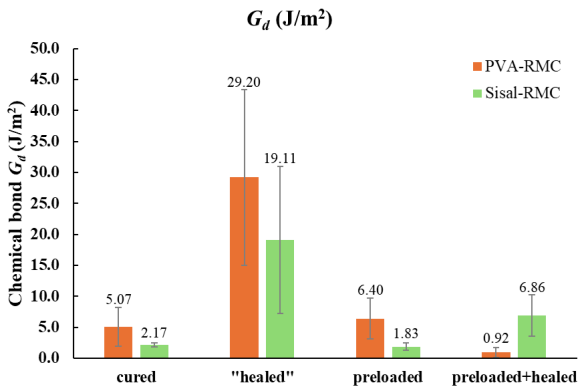


**Figure 3**: Chemical bond of Sisal-RMC and PVA-RMC specimens

Figure 4 presents the frictional bond $\tau_o$ and the trends observed mirror those in Figure 3, except for the preloaded-and-healed specimens wherein the PVA-RMC has a higher $\tau_o$ value than Sisal-RMC. Additionally, both preloaded-and-healed PVA-RMC and Sisal-RMC have a higher $\tau_o$ than their cured counterparts, indicating that alternating water/$CO_2$ conditioning can recover frictional bond strength for both fiber types. The healing-induced recovery of $\tau_o$ has also been observed in PVA-PC specimens [12].

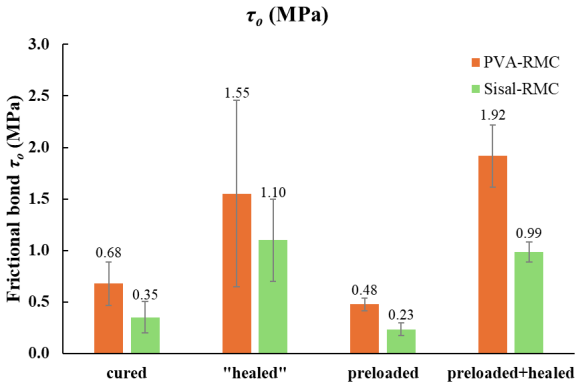


**Figure 4**: Frictional bond of Sisal-RMC and PVA-RMC specimens

Figure 5 shows the energy absorbed per fiber surface area to achieve 1mm displacement during the pullout process $G_{w\_1.0}$. The PVA-RMC specimens consistently have higher $G_{w\_1.0}$ than Sisal-RMC specimens, which suggests a stronger bond between the PVA fiber and the RMC matrix compared to sisal fiber. Additionally, the alternating water/$CO_2$ conditioning increased the energy absorption of both the preloaded and non-preloaded specimens.

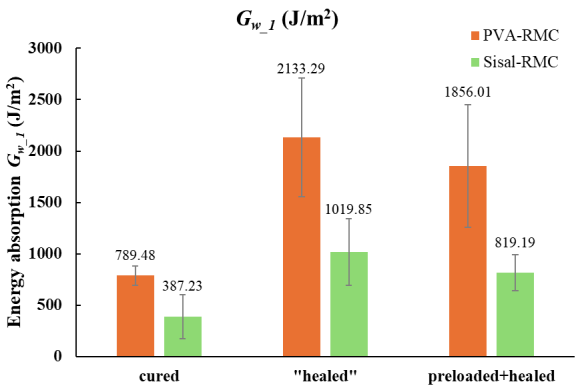


**Figure 5**: Energy absorbed per interface area of Sisal-RMC and PVA-RMC specimens

Finally, Figure 6 presents the slip-hardening coefficient $\beta$, which is a measure of the increased in frictional resistance against fiber-pullout load. The Sisal-RMC specimens initially display a higher $\beta$ in the cured state compared to PVA, potentially due to the natural roughness and surface texture of sisal fibers which might provide better mechanical interlocking as it is being abraded during the slippage stage. For the PVA-RMC specimens, the increase from the cured to the healed state suggests that the healing process may enhance the interfacial bond or texture between the fiber and the matrix, leading to improved slip-hardening. However, the reduction in $\beta$ after preloading-and-healing in both types of fibers indicates that the healing processes might not fully restore the interfacial properties damaged during initial loading. This is particularly pronounced in natural fibers, which might undergo more substantial structural changes due to their hygroscopic nature and organic composition. The variability in $\beta$ for Sisal-RMC across conditions suggests a less consistent interface property, which might be due to the variable nature of natural fibers and their interaction with the matrix.

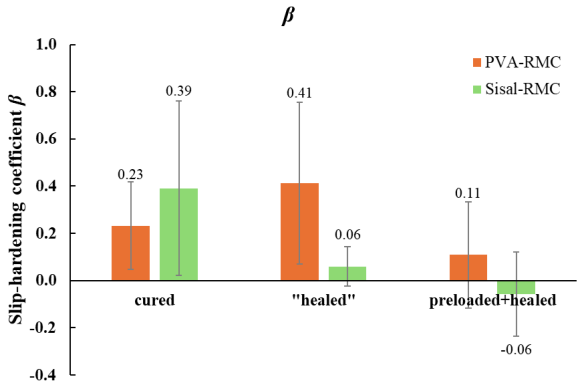


**Figure 6**: Slip-hardening coefficient of Sisal-RMC and PVA-RMC specimens

The normalized interface properties, calculated by dividing the interface properties by those of the cured specimens, are presented in Table 3. The results show that Sisal-RMC has a better recovery of both the chemical and frictional bond, while PVA-RMC has a better recovery of energy absorption capability. The normalized interface property of the preloaded-and-healed PVA-RMC is less than one, which implies that the chemical bond cannot be fully recovered. The negative $\beta$ of Sisal-RMC after preloading-and-healing suggests that the fiber may have been severely damaged during preloading, which affected its ability to increase the frictional resistance during slippage. Therefore, the healing process in Sisal-RMC and PVA-RMC impacts the interface properties differently, reflecting the influence of fiber types and their interactions with the matrix.

**Table 3**: Normalized interface properties

| Specimen | Group | $G_d$ (J/m$^2$) | $\tau$ (MPa) | $G_{w\_1.0}$ (J/m$^2$) | $\beta$ |
|---|---|---|---|---|---|
| Sisal-RMC | "healed" (not preloaded) | 8.81 | 3.14 | 2.63 | 0.15 |
| | preloaded and healed | 3.16 | 2.83 | 2.12 | -0.15 |
| PVA-RMC | "healed" (not preloaded) | 5.76 | 2.28 | 2.7 | 1.78 |
| | preloaded and healed | 0.18 | 2.82 | 2.35 | 0.48 |

*values are divided by the interface property after curing

## 4 CONCLUSIONS

This work investigated the use of alternating water/$CO_2$ conditioning to promote interface healing in RMC specimens with different fiber types, particularly natural fiber and synthetic fiber. The results indicate significant differences in how synthetic and natural fibers interact with the RMC matrix and respond to water/$CO_2$ conditioning. PVA fibers bond more effectively with the RMC matrix, possibly due to better chemical compatibility. On the other hand, sisal fibers, being organic and dimensionally unstable, do not bond as effectively with the matrix. Additionally, both Sisal-RMC and PVA-RMC can benefit from the healing process involving alternating water/$CO_2$ conditioning, but the interface properties are influenced differently. These differences highlight the role of fiber properties in determining the interfacial bond characteristics and the effectiveness of healing processes.

Hence, it is important to consider fiber type in the design and application of FRCCs,

particularly in scenarios where autogenous healing is critical to the material's performance and durability. Further research into optimizing the healing process could enhance the performance of both natural and synthetic FRCCs, expanding their application in sustainable construction.

## REFERENCES


[1] G. Fischer, V.C. Li, Effect of fiber reinforcement on the response of structural members, Engineering Fracture Mechanics 74 (2007) 258–272. https://doi.org/10.1016/j.engfracmech.2006.01.027.

[2] Z. Lin, T. Kanda, V.C. Li, On Interface Property Characterization and Performance of Fiber Reinforced Cementitious Composites, Concrete Science and Engineering 1 (1999) 173–174.

[3] K. Van Tittelboom, N. De Belie, Self-Healing in Cementitious Materials—A Review, Materials 6 (2013) 2182–2217. https://doi.org/10.3390/ma6062182.

[4] A. Célino, S. Freour, F. Jacquemin, P. Casari, The hygroscopic behavior of plant fibers: a review, Frontiers in Chemistry 1 (2014). https://www.frontiersin.org/articles/10.3389/fchem.2013.00043 (accessed July 24, 2022).

[5] R. Santos, P. Lima, Effect of Treatment of Sisal Fiber on Morphology, Mechanical Properties and Fiber-Cement Bond Strength, Key Engineering Materials 634 (2015) 410–420. https://doi.org/10.4028/www.scientific.net/KEM.634.410.

[6] V.C. Li, C. Wu, S. Wang, A. Ogawa, T. Saito, Interface Tailoring for Strain-Hardening Polyvinyl Alcohol-Engineered Cementitious Composite (PVA-ECC), MJ 99 (2002) 463–472. https://doi.org/10.14359/12325.

[7] C. Unluer, 7 - Carbon dioxide sequestration in magnesium-based binders, in: F. Pacheco-Torgal, C. Shi, A.P. Sanchez (Eds.), Carbon Dioxide Sequestration in Cementitious Construction Materials, Woodhead Publishing, 2018: pp. 129–173. https://doi.org/10.1016/B978-0-08-102444-7.00007-1.

[8] R. Hay, K. Celik, Hydration, carbonation, strength development and corrosion resistance of reactive MgO cement-based composites, Cement and Concrete Research 128 (2020) 105941. https://doi.org/10.1016/j.cemconres.2019.105941.

[9] L. Pu, C. Unluer, Investigation of carbonation depth and its influence on the performance and microstructure of MgO cement and PC mixes, Construction and Building Materials 120 (2016) 349–363. https://doi.org/10.1016/j.conbuildmat.2016.05.067.

[10] B. Wu, J. Qiu, Incorporating hollow natural fiber (HNF) to enhance CO2 sequestration and mechanical properties of reactive magnesia cement (RMC)-based composites: Feasibility study, Journal of CO2 Utilization 57 (2022) 101874. https://doi.org/10.1016/j.jcou.2021.101874.

[11] B. Wu, P. Wang, J. Qiu, Autogenous healing of the interface between hollow natural fiber (HNF) and reactive magnesia cement (RMC) matrix, Construction and Building Materials 422 (2024) 135843. https://doi.org/10.1016/j.conbuildmat.2024.135843.

[12] J. Qiu, S. He, E.-H. Yang, Autogenous healing and its enhancement of interface between micro polymeric fiber and hydraulic cement matrix, Cement and Concrete Research 124 (2019) 105830. https://doi.org/10.1016/j.cemconres.2019.105830.

[13] J. Qiu, S. Ruan, C. Unluer, E.-H. Yang, Autogenous healing of fiber-reinforced reactive magnesia-based tensile strain-hardening composites, Cement and Concrete Research 115 (2019) 401–413. https://doi.org/10.1016/j.cemconres.2018.09.016.

[14] S. Ruan, J. Qiu, E.-H. Yang, C. Unluer, Fiber-reinforced reactive magnesia-based tensile strain-hardening composites, Cement and Concrete Composites 89 (2018) 52–61. https://doi.org/10.1016/j.cemconcomp.2018.03.002.

[15] C. Redon, V.C. Li, C. Wu, H. Hoshiro, T. Saito, A. Ogawa, Measuring and Modifying Interface Properties of PVA Fibers in ECC Matrix, Journal of Materials in Civil Engineering 13 (2001) 399–406. https://doi.org/10.1061/(ASCE)0899-1561(2001)13:6(399).

[16] Y. Liu, B. Wu, J. Qiu, A new fiber-bridging constitutive model for quantifying the matrix carbonation and fiber-to-matrix interface healing in PVA fiber-reinforced SHCC, Construction and Building Materials 399 (2023) 132548. https://doi.org/10.1016/j.conbuildmat.2023.132548.